

Full Length Research Paper

CuIn (Se,S)₂ based photovoltaic cells from one-step electrodeposition

C. Sene^{1*}, B. Ndiaye¹, M. Dieng¹, B. Mbow¹ and H. Nguyen Cong²

¹Laboratoire des Semi-conducteurs et d'Energie Solaire (LASES), Université Cheikh Anta Diop, Dakar, Sénégal.

²Laboratoire d'Electrochimie et de Chimie Physique du Corps Solide, UMR 7177, CNRS-Université Louis Pasteur, 4 rue Blaise Pascal, 67000 Strasbourg France".

Accepted 19 August, 2009

The formation of CuIn (Se,S)₂ films for application in photovoltaic devices by post-deposition treatments of electrodeposited pre-cursors is described. The polycrystalline CuInSe₂ (CIS) pre-cursor layers were prepared by the one-step electrodeposition (ED) method on molybdenum-coated soda lime (SL) glass substrates. Growth was performed from low concentration buffered baths containing CuSO₄, In₂(SO₄)₃ and SeO₂ with Li₂SO₄ electrolyte. As deposited films were amorphous and required recrystallization by annealing in H₂Se or H₂S prior to device processing. Reaction in flowing H₂Se produced random oriented CuInSe₂ films which resulted in devices with low conversion efficiencies of only ~3%. Annealing in flowing H₂S led to partial replacement of the selenium in the CuInSe₂ film with sulfur, determined by XRD and EDS to produce CuIn(Se,S)₂ quaternary alloys. Devices processed from CuIn(Se,S)₂ films showed improved J-V characteristic with conversion efficiencies of ~6.4%.

Key words: CuInSe₂, CuIn(Se,S)₂, absorber layers, electrodeposition, pHydron buffer, photovoltaic cells.

INTRODUCTION

The development of thin film solar cells using CuInSe₂ and its gallium and/or sulfur containing alloys as the absorber layer has given rise to significant progress in device performances. These alloying processes allow widening of the optical band gap of the chalcopyrite absorber materials and therefore increasing of the open-circuit voltage (V_{oc}). Incorporation of gallium into CuInSe₂ films to form Cu(In,Ga)Se₂ (CIGS) has resulted in higher performing devices reaching almost 20% conversion efficiency (Contreras et al., 2005). However, the increase of V_{oc} with the energy band gap E_g , by Ga incorporation is not linear and resulted in a device performance decrease for E_g above 1.3 eV corresponding to Ga/(In+Ga) higher than 0.5 (Contreras et al., 2005; Shafarman et al., 1996; Yamada et al., 2004; Rau et al., 2001). Graded Cu(In,Ga)(Se,S)₂ films have been investigated by many research groups (Ennaoui, 2000; Alberts et al., 2004;

Taunier et al., 2005) and photovoltaic devices processed with these absorber layers. In the device designed by Siemens Solar Industries, Ga is accumulated at the back contact region giving a high back surface field while the surface region is alloyed with S to increase V_{oc} (Tarrant et al., 1996). The formation of CuIn(Se_{1-y},S_y)₂ by reaction of Cu-In precursors in H₂Se and H₂S gas mixture has been discussed (Sheppard and Alberts 2006). The reaction of CuInSe₂ films in a H₂S atmosphere to form CuIn(Se_{1-y},S_y)₂ have been investigated with focus on the interdiffusion of Se and S in the material lattice and band gap widening. By treating CIS single crystals in H₂S atmosphere at 575 °C, Titus et al. (2006) modeled the incorporation of sulfur by a chalcogene exchange reaction at the crystal surface followed by diffusion in the crystal lattice, determining a lattice diffusion coefficient D_1 of about 10^{-16} cm².s⁻¹. The mechanism is then supposed to be active in polycrystalline CIS films, allowing enhanced sulfur incorporation, via diffusion along the grain boundaries. A method for making thin polycrystalline CuIn(Se_{1-y},S_y)₂ films with uniform or graded composition has also been developed and a model which

*Corresponding author. E-mail: chksene@yahoo.fr. Tel: 33.825.02.02. Fax : 33.8246318.

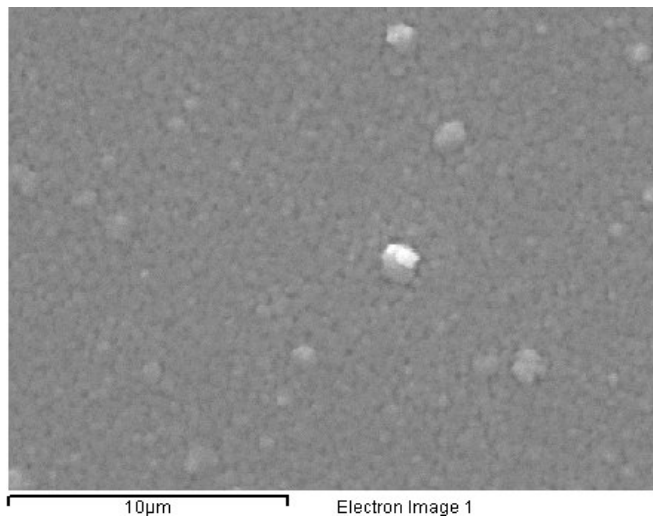


Figure 1a. SEM micrographs of a CIS film deposited from buffered bath: the as-deposited film.

estimates the bulk and grain boundary diffusion established by Engelmann et al. (2001). These authors have shown that the use of a H_2S/H_2Se gas mixture allows controlling the S/Se composition of either a graded or uniform film which can then be used to tailor the band gap of the material. Sulfur treatments of CIS crystals led to the formation of a higher band gap surface region on CIS monograin layers (Altosaar et al., 2005).

In a previous paper (Sene et al., 2006), one step electrodeposition of polycrystalline $CuInSe_2$ films from low concentration buffered deposition baths has been discussed. Electrodeposition is known to be a convenient method for the development of low cost materials for photovoltaic device processing. This material processing could be more appealing with the use of a buffer since with the addition of the buffer species, electrochemical baths become more stable during deposition and remain stable over a time period of weeks. However, deposition from buffered solutions gave CIS absorber layers resulting in solar cell devices with low open-circuit voltage and efficiency (Sene et al., 2006). One possibility for increasing the open-circuit voltage in these devices is to use an absorber layer of material with a higher band gap.

This could be achieved by reacting the CIS films in H_2S atmosphere to form a heterojunction interface with a uniform or graded layer. In the current paper we describe the processing and characterization of $CuIn(Se,S)_2$ films for photovoltaic application by annealing as grown ED CIS samples in a flowing H_2S/Ar atmosphere at $500^\circ C$ to partially substitute Se by S.

Experimental details

$CuInSe_2$ films with a thickness of approximately $2 \mu m$ were electrodeposited using a Princeton Applied Research (PAR) Poten-

tiostat/Galvanostat Model 173 and a three-electrode cell set-up with a Pt mesh counter electrode and a saturated calomel electrode (SCE) reference electrode. The working electrode was a $1'' \times 1''$ dc-sputtered $0.7 \mu m$ Mo coated soda-lime glass.

The Mo-coated glass substrates were washed prior to CIS growth in water containing detergent (liquinox) and then sufficiently rinsed with deionized water. All chemicals, copper(II) sulfate pentahydrate, $CuSO_4 \cdot 5H_2O$, indium (III) sulfate hydrate $In_2(SO_4)_3 \cdot H_2O$, selenium dioxide, SeO_2 and lithium sulfate hydrate, $Li_2SO_4 \cdot H_2O$, were received from Aldrich and used without purification. Film deposition was carried out from a $500 cm^3$ acidic aqueous electrochemical bath containing $CuSO_4 \cdot 5H_2O$, $In_2(SO_4)_3 \cdot H_2O$ and SeO_2 with $Li_2SO_4 \cdot H_2O$ added as a supporting electrolyte. The electrochemical solution was buffered with a pH = 3 Hydron buffer, a mixture of sulphamic acid and potassium biphthalate, giving a bath pH ~ 2.5 . The use of buffer allows to control the pH of the deposition bath and to reduce the occurrence of oxides or hydroxides precipitation in the solution (Fernandez and Bhattacharya, 2005). The applied potential used for depositing the CIS films was $-0.55 V/SCE$. All growth experiments were performed at room temperature with a slow stirring of the bath. Approximately $2 \mu m$ thick CIS layers were obtained for 90 - 100 min deposition. Full details of bath and deposition conditions have been given elsewhere (Sene et al., 2006). On completion of growth, CIS films were removed from the bath, rinsed with deionized water and dried in an argon stream.

The post-deposition treatments of the CIS films were then carried out at $500^\circ C$ in either 0.35% $H_2Se/Ar(g)$ or 0.35% $H_2S/Ar(g)$ (Scott Specialty Gases) atmosphere for 20 min in a horizontal laminar flow CVD reactor at atmospheric pressure as described elsewhere (Engelmann et al., 2001).

Surface morphology was characterized by an Amray 1810 T scanning electron microscope (SEM). The composition of the reacted films was measured by an Oxford Instrument Energy 200 energy dispersive x-ray spectroscopy (EDS) at 20 kV with a vertically incident beam using an Oxford INCA system mounted to the Amray 1810 T SEM and evaporated $Cu(In,Ga)Se_2$ films as standards. X-ray diffraction (XRD) experiments were carried out using a Philips/Norelco diffractometer with Bragg-Brentano focusing geometry and $CuK\alpha$ radiation at 35 kV. The optical transmittance and reflectance of the films were measured using Perkin-Elmer Lambda-9 UV-visible-IR Spectrophotometer fitted with integrating sphere.

Solar cell devices were completed according to the standard solar cell fabrication described by Shafarman et al. (1996). The process includes a chemical bath deposited CdS buffer layer, a sputtered intrinsic ZnO and a doped highly-conductive AlO_2 -doped ZnO window layer and a Ni-Al grid. J-V curves were recorded under AM 1.5 ($100 mW \cdot cm^{-2}$) sun simulation at $25^\circ C$ using an Oriel Xenon solar simulator on $0.47 cm^2$ area.

RESULTS AND DISCUSSION

Morphological characterization

The morphology of the films was investigated by SEM. Figures 1 and 2 depict the SEM micrograph pictures of the representative CIS samples as-deposited and following annealing in H_2Se/Ar and H_2S/Ar , respectively. The as-deposited film surfaces (Figure 1a and Figure 2a) are composed of small particles of approximately $0.5 \mu m$ in size with some scattered larger particles ($1.2 \mu m$ average size) embedded in the surface. The film surfaces

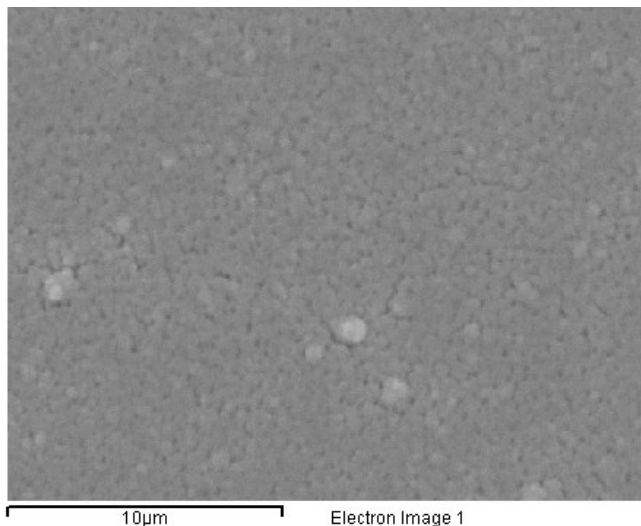


Figure 1b. SEM micrographs of a CIS film deposited from buffered bath: after its post-selenization.

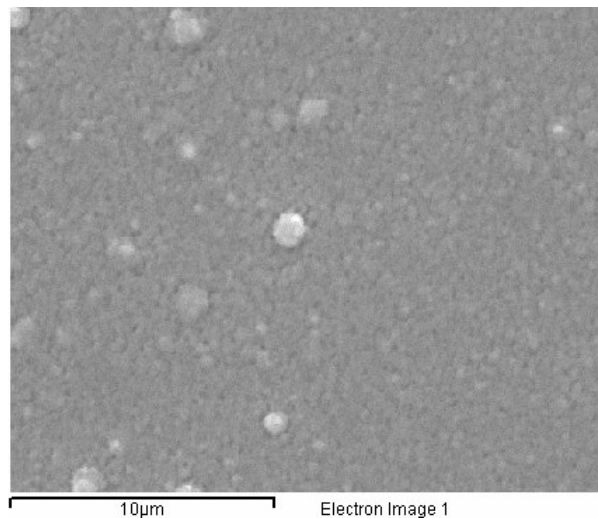


Figure 2a. SEM micrographs of a CIS film deposited from buffered bath: the as-deposited film.

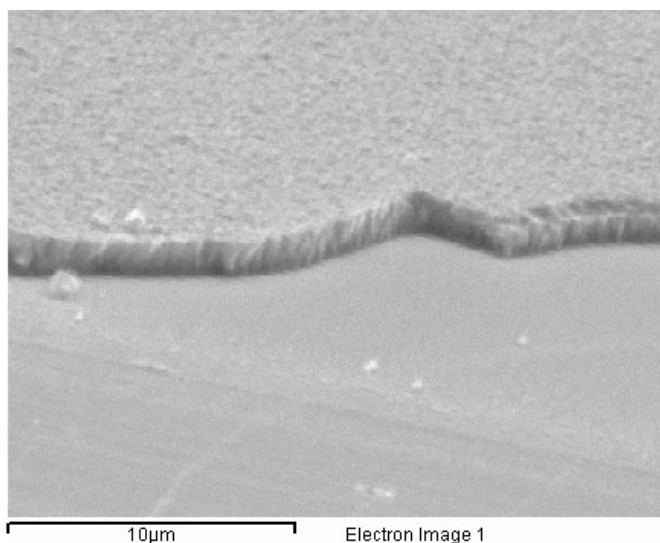


Figure 1c. SEM micrographs of a CIS film deposited from buffered bath: cross-section image of an as-deposited film.

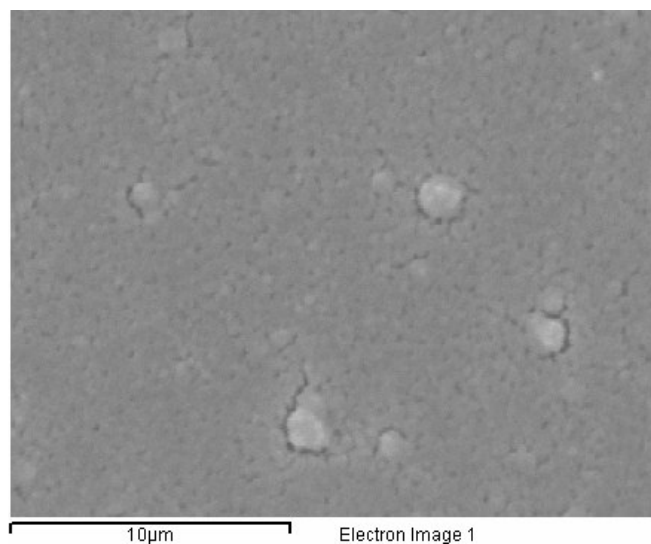


Figure 2b. SEM micrographs of a CIS film deposited from buffered bath: after its post-sulfurization.

of the two samples are identical, indicating that the surface morphology of CIS films grown from buffered baths is very reproducible. Such morphology has not been observed for CIS films grown from a non-buffered bath (Sene et al., 2006) and has been explained as being probably the result of the buffer species either slowing diffusion of electro-active species to the surface of the electrode or being surface-active and affecting film growth by adsorption on the growing CIS particles. However, these effects do not change the chemical mechanism of the film growth or the composition of the deposited film (Sene et al., 2006).

Figure 1c shows a cross section SEM image of an as-deposited film, showing the grain structure of the layer.

The grains are small, about 0.4 - 0.5 μm in size, and appeared columnar.

After reaction of the films in 0.35% H₂Se/Ar(g) atmosphere for 20 min, no or only minor changes have been observed in surface morphology of the CIS layers (Figure 1b compared to Figure 1a). In contrast, reaction of the films in 0.35% H₂S/Ar(g) for the same duration led to a surface morphology with slightly larger particle sizes (Figure 2b compared to Figure 2a). It appears that small surface particles in the as-deposited films merged into each other by H₂S-sulfurization resulting in smoother CuIn(Se,S)₂ surface film. In both cases however, some degree of cracking is observed, particularly around the larger particles.

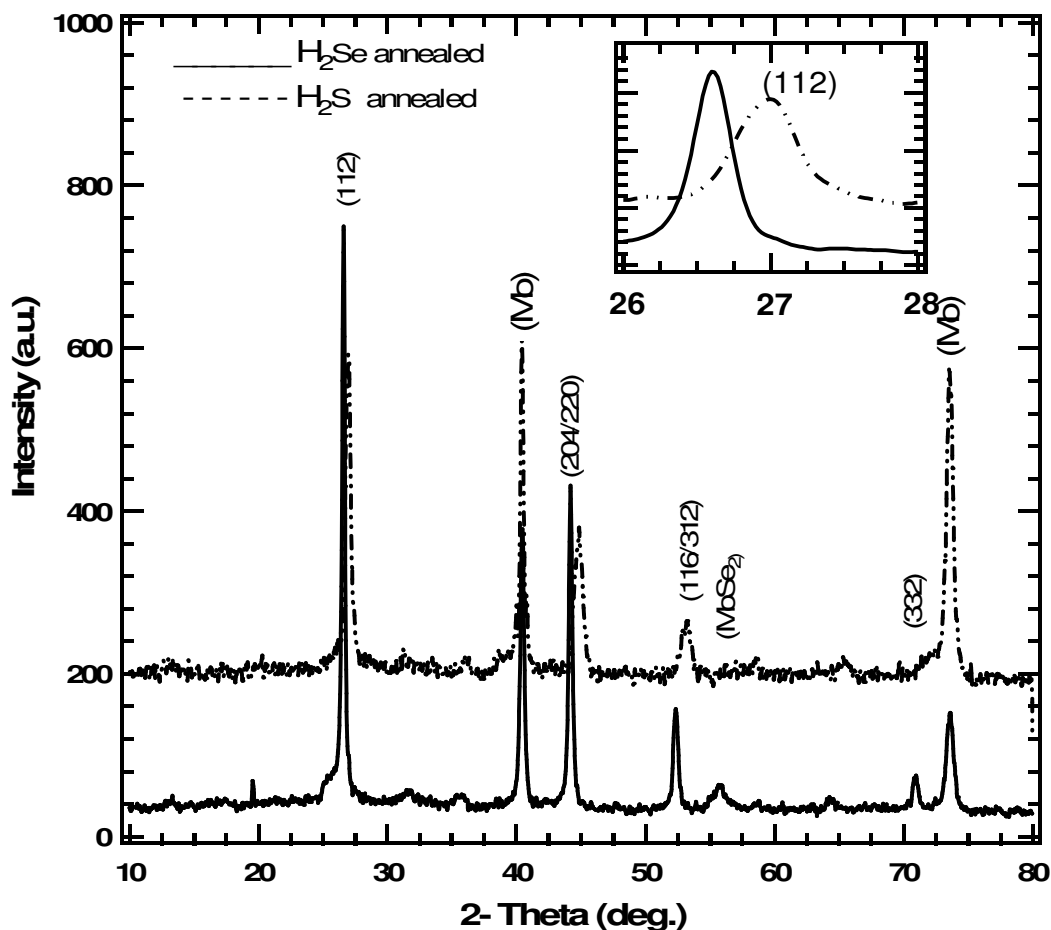


Figure 3. XRD spectra of two CIS films deposited from a buffered bath and heat treated in $\text{H}_2\text{Se}/\text{Ar}(\text{g})$ and $\text{H}_2\text{S}/\text{Ar}(\text{g})$ atmosphere.

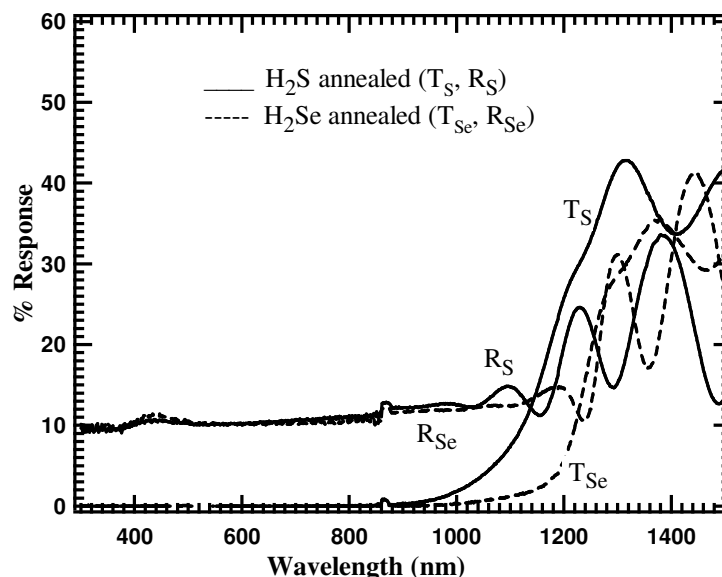
X-ray diffraction (XRD) analysis

We have previously reported XRD patterns of CuInSe_2 films electrodeposited from buffered baths (Sene et al., 2006), which showed weak and broad peaks characteristics of CIS chalcopyrite phases, but indicating the as-deposited films consist of a high degree of amorphous or microcrystalline phase. The x-ray diffractograms of post-selenized and post-sulfurized CIS samples are shown in Figure 3. Both XRD patterns show sharp and well defined peaks indicating that recrystallization occurred during the post-deposition heat treatments of the films and identify approximately random oriented crystals (Sene et al., 2006). The H_2Se -selenized samples show almost pure CIS, by the characteristic (112), (204,220), (116,312), and (332) reflections of the tetragonal structure (see JCPDS 35 - 1102 powder diffraction files). The additional peaks are attributed to Mo and in the case of the H_2Se -selenized films, to MoSe_2 , which forms on reaction with H_2Se at temperatures higher than 450°C . After sulfurization in $\text{H}_2\text{S}/\text{Ar}$ atmosphere, the characteristic chalcopyrite

reflections are slightly shifted towards the higher 2θ values, indicating probably the existence of the phase $\text{CuIn}(\text{Se},\text{S})_2$ (JCPDS 35 - 1102). This is most evidenced from the inset of Figure 3 which highlights the shift of the (112) reflection from $2\theta = 26.600^\circ$; $d = 3.348$ to $2\theta = 26.980^\circ$; $d = 3.302$, by the sulfur incorporation. This shift corresponds to a sulfur level in the CIS sample of 11.47% as indicated by EDS results summarized in Table 1. Using Cu-poor CIS films on soda lime glass substrates, Titus et al. (2001) observed a slight shift of the (112) CuInSe_2 peak and highlighted a (112) CuInS_2 peak. GIXRD analysis revealed that CuInS_2 tended to accumulate as a surface layer. AES depth profiles measured on Cu-poor CIS samples reacted in H_2S atmosphere, shows that sulfurized crystals contain a region of high S content at the surface and remain essentially S-free deep in their bulk (Titus et al., 2006). All our as-deposited films were slightly copper poor as can be seen in the EDS results summarized in table 1. They should therefore contain high S content at their surface after reaction in H_2S atmosphere, according to above mentioned results.

Table 1. Composition of CIS films deposited from buffered baths before and after heat treatment in H₂Se and H₂S atmospheres.

As-deposited film composition (at. %)			Annealed film composition (at. %)				
Cu	In	Se	Annealing atmosphere	Cu	In	Se	S
22.18	23.25	54.58	0.35% H ₂ Se/Ar(g)	24.05	24.68	51.27	0
22.32	23.46	54.22	0.35% H ₂ S/Ar(g)	23.95	24.98	39.60	11.47

**Figure 4.** Transmission (T_{Se} , T_S) and reflection (R_{Se} , R_S) spectra of post-selenized and post-sulfurized CuInSe₂ samples.

Optical properties

Optical transmittance and reflectance were measured on post-selenized and post-sulfurized ED-CIS samples to evaluate their optical band gaps and absorption coefficients. In fact, near the fundamental absorption edge of semiconductor films there is a dependence of absorption coefficient on the photon energy. This relationship in the high absorption region is as follows:

$$\alpha = \frac{A^*(h\nu - E_g)^n}{h\nu}$$

Where

α = The absorption coefficient of the semiconductor material;

$h\nu$ = The photon energy (eV);

ν = The light frequency;

h = Planck's constant

E_g = The optical energy band gap;

A a constant which is related to the effective masses of electrons and holes in the bands of the material and n

is a constant associated with the absorption mechanism of the film. For a direct allowed transition n has the value 1/2 and the plot of $(\alpha h\nu)^2$ versus photon energy $h\nu$ forms a straight line whose intercept with the $\alpha = 0$ axis yields the value of the direct energy band gap of the material, E_g .

In addition, from the transmission and reflection spectra one can get the value of the absorption coefficient α through the well-known relation:

$$\alpha = \frac{1}{d} \ln \left[\frac{100 - R\%}{T\%} \right]$$

$T\%$ and $R\%$ are the transmittance and the reflectance of the samples respectively.

Figure 4 depicts the transmission and reflection spectra of both post-selenized and post-sulfurized CIS samples. We observed a sharp fall at the band gap edge of both samples. One can furthermore note from the relative difference of the two films, that the H₂S-sulfurized sample exhibits an onset of absorption at lower photon wavelengths than does the H₂Se-selenized sample.

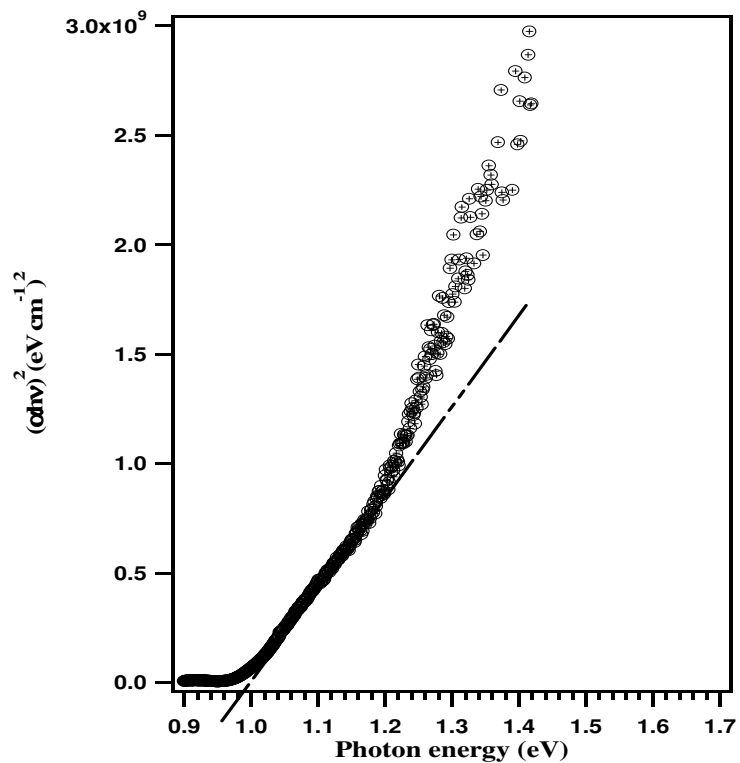


Figure 5a. Plots of $(\alpha h\nu)^2$ versus $h\nu$ for post-selenized CuInSe_2 samples.

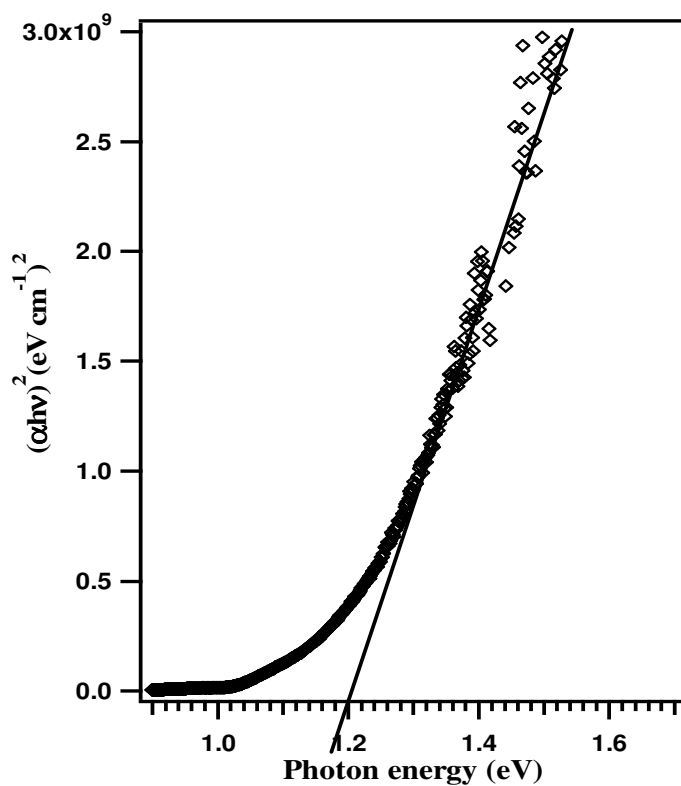
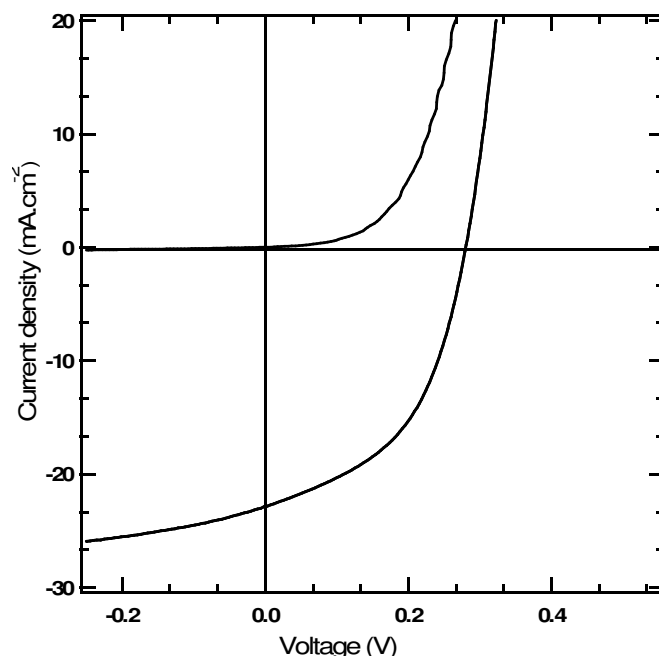


Figure 5b. Plots of $(\alpha h\nu)^2$ versus $h\nu$ for post-sulfurized CuInSe_2 samples.

Table 2. PV parameters of solar cell devices measured under AM 1.5 conditions.

Post-deposition treatment of the absorber layer	V_{oc} (V)	J_{sc} (mA.cm ⁻²)	FF (%)	η (%)
Device with selenized CIS film	0.2806	22.88	47.9	3.07
Device with sulfurized CIS film	0.3932	28.20	57.50	6.37

**Figure 6a.** J-V curves of solar cell devices processed with CIS films deposited from a buffered baths: device processed with post-selenized film.

The band gap energies of the samples are determined from the curves shown in Figures 5. The straight line fits indicate that the optical transition is direct. The band gap of the H₂Se-selenized CIS film (Figure 5a) is the range of 1.00 eV while that of the H₂S-sulfurized sample lies in the range 1.20 eV (Figure 5b). The high S content at the H₂S-sulfurized surface film is responsible of the optical band gap of the material increase since CuInSe₂ and CuInS₂ have optical band gaps of 1.02 and 1.53 eV respectively. Such E_g value has been interpreted as the mean value of the material band gap when considering an almost Se free surface film.

Solar cells analysis

Figure 6 shows the current density vs. voltage (J-V) characteristics of the CIS based solar cell devices processed from H₂Se/Ar(g) and H₂S/Ar(g) treated electrodeposited precursor films, measured in the dark and under the standardized AM 1.5 global spectrum

on 0.47 cm² cells. Table 2 lists the photovoltaic cell parameters. The open-circuit voltage of the device processed with the sulfurized film is 112.6 mV higher than that of the device processed with the selenized film, and the short-circuit current density is also increased by 5.32 mA/cm². The conversion efficiencies of these H₂Se/Ar(g)- and H₂S/Ar(g)-treated devices are 3.1 and 6.4%, respectively. The higher performance of the devices processed from the sulfurized film is due to improvements in V_{oc} and J_{sc} and could be, in part, explained by an increase in the optical band gap of the absorber material as a result of the sulfur incorporation. Improved structural and morphological properties of the samples following the reaction of the film in H₂S/Ar(g) atmosphere may also account for the observed improvements including the observed decrease in device shunting. The influence of morphological and structural properties of the absorber layers on the conversion efficiencies of the completed cells are clearly reflected in the J-V curves of the devices.

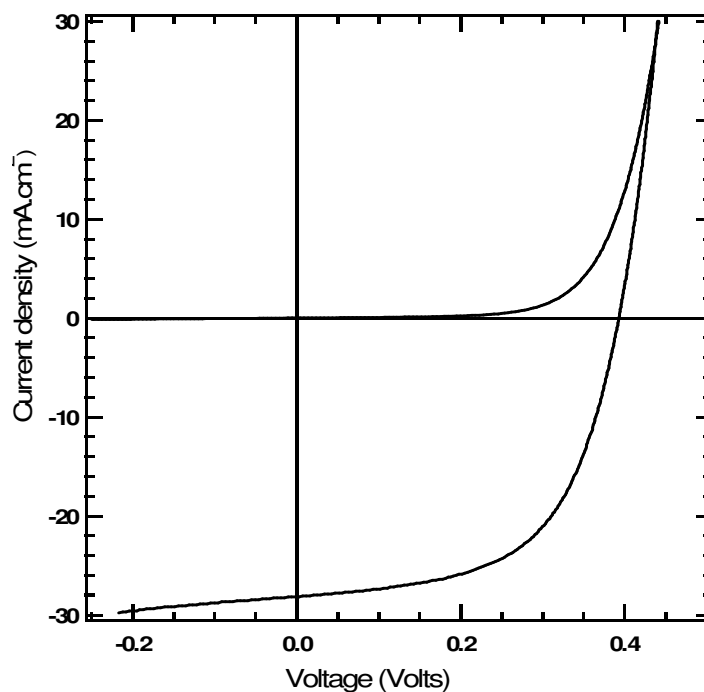


Figure 6b. J-V curves of solar cell devices processed with CIS films deposited from a buffered baths: device processed with post-sulfurized film.

Conclusion

Buffering the electrolytic bath with a pHDrion pH = 3 buffer stabilizes the CuInSe_2 deposition solution, but produces absorber layers which result in photovoltaic devices of lower conversion efficiencies. We have shown in this investigation that the incorporation of sulfur into these layers by reaction in H_2S atmosphere resulted in improvement of the structural and optoelectronic properties of the films and led therefore to devices with higher conversion efficiencies.

ACKNOWLEDGEMENTS

This work has been supported in part by the J. William Fulbright Foreign Scholarship Board and the Bureau of Educational and Cultural affairs, United States Department of State. One of the authors, Dr. C. Sene is grateful to IEC staff members: S. Hegedus, W. N. Shafarman, B. E. McCandless for valuable technical discussions, Estela Calixto and Greg Hanket for post deposition treatments and R. Dozier for solar cells characterizations.

REFERENCES

Alberts V, Titus J, Birkmire RW (2004). "Material and Device Properties of Single-Phase $\text{Cu}(\text{In,Ga})(\text{Se,S})_2$ Alloys Prepared by Selenization/Sulfurization of Metallic Alloys", *Thin Solid Films* 207: 451-452.

- Altosaar M, Danielson M, Kauk M, Krustok J, Mellikov E, Raudoja J, Timmo K, Varema T (2005). "Further developments in CIS monograin layer solar cells technology" *Sol. Energy Mater. Sol. Cells* 87: 25.
- Contreras MA, Ramanathan K, AbuShama J, Hasoon F, Young DL, Egaas B, Noufi R (2005). "Diode characteristics in state-of-the-art $\text{ZnO/CdS/Cu}(\text{In}_{1-x}\text{Ga}_x)\text{Se}_2$ solar cells", *Prog. Photovolt. Res. Appl.* 13- 209.
- Engelmann M, McCandless BE, Birkmire RW (2001). "Formation and Analysis of Graded $\text{CuInSe}_{1-y}\text{S}_y$ Films", *Thin Solid Films* 387: 14.
- Ennaoui A (2000). "High Efficiency CIGSS Thin Film based Solar Cells and Mini-modules", *M. J. Condensed Matter* 3(1): 8-15.
- Fernandez AM, Bhattacharya RN (2005). "Electrodeposition of $\text{CuIn}_{1-x}\text{Ga}_x\text{Se}_2$ precursor films: optimization of film composition and morphology", *Thin Solid Films* 474: 10.
- Rau U, Schmidt M, Jasenek A, Hanna G, Schock HW (2001). "Electrical characterization of $\text{Cu}(\text{In,Ga})\text{Se}_2$ thin-film solar cells and the role of defects for the device performance", *Sol. Energy Mater. Sol. Cells* 67-137.
- Sene C, Dobson KD, Calixto EM, Birkmire RW (2008). "Electrodeposition of CIS Absorber Layers from Buffered and Non-Buffered Sulfate-Based Solutions", *Thin Solid Films*, 516: 2188-2194.
- Shafarman WN, Klenk R, McCandless BE (1996). "Device and Material Characterization of $\text{Cu}(\text{In,Ga})\text{Se}_2$ Solar Cells with Increasing Band Gap", *J. Appl. Phys.* 79(9): 7324.
- Sheppard J, Alberts V (2006). "Deposition of single-phase $\text{CuIn}(\text{Se,S})_2$ thin films from the sulfurization of selenized CuIn alloys", *J. Phys. D: Appl. Phys.* 39: 3760-3763.
- Tarrant DE, Bauer J, Dearmore R, Dietrich ME, Fernandez GT, Frausto OD, Fredric CV, Jensen CL, Ramos AR, Schmitzberger JA, Wieting R (Ed), Willett D, Gay RR (1996). "Progress in CIS-based module development", *NREL/SNL PV Program Review*, AIP Conf. Proc. 394:143.
- Taunier S, Sixx-Kurdi J, Grand PP, Chomont A, Ramdani O, Parissi L, Panheleux P, Naghavi N, Hubert C, Ben-Farah M, Fauvarque JP, Connolly J, Roussel O, Mogensen P, Mahe E, Guillemoles JF, Lincot D, Kerrec O (2005). " $\text{Cu}(\text{In,Ga})(\text{S,Se})_2$ solar cells and modules by

- electrodeposition", *Thin Solid Films* 526: 480-481.
- Titus J, Birkmire RW, Hack C, Müller G, McKeown P (2006). "Sulfur Incorporation into Copper Indium Diselenide Single Crystals Through Annealing in Hydrogen Sulfide", *J. Appl. Phys.* 99: 043502.
- Titus J, Schock HW, Birkmire RW, Shafarman WN, Singh UP (2001). "Post-Deposition Sulfur Incorporation into CuInSe_2 Thin Films" *Proc. Mat. Res. Soc. Symp.* 668: H1.5.1.
- Yamada A, Matsubara K, Sakurai K, Ishizuka S, Tampo H, Fons PJ, Iwata K, Niki S (2004). "Effect of band offset on the open circuit voltage of heterojunction $\text{CuIn}_{1-x}\text{Ga}_x\text{Se}_2$ solar cells", *Appl. Phys. Lett.* 85: 5607.